

Loss of VOPP1 overexpression in squamous carcinoma cells induces apoptosis through oxidative cellular injury

Alexander S Baras¹, Alex Solomon², Robert Davidson¹ and Christopher A Moskaluk^{1,3}

The *vesicular overexpressed in cancer prosurvival protein 1 (VOPP1)* gene product (previously known as GASP and ECOP) has a poorly characterized functional role in cancer cells, although its expression levels are known to be elevated in many cancer types. To determine the role that VOPP1 has in human squamous cell carcinoma (SCC), a series of siRNA-mediated expression knockdown experiments were performed in carcinoma-derived model systems with confirmed endogenous VOPP1 overexpression (three SCC-derived cell lines: SCC-9, FaDu, and H2170, as well as the cervical adenocarcinoma HeLa cell line, which has been examined in relevant previous reports). The data indicate that VOPP1 knockdown induces cell death at 72 h post-transfection and this is caused by the induction of apoptosis via the intrinsic pathway. Analysis of microarray gene expression profiling showed that genes whose expression was affected by VOPP1 knockdown exhibited enrichment in annotations of oxidative stress and mitochondrial dysfunction. Reporters of reactive oxygen species (ROS) and mitochondrial membrane potential show that ROS levels become elevated and mitochondrial dysfunction occurs with VOPP1 knockdown at time points before the activation of effector caspases and cell death seen at later time points. Furthermore, the introduction of the antioxidant *N*-acetyl cysteine was able to abrogate the induction of apoptosis observed with VOPP1 knockdown in a dose-responsive manner. Reporter constructs for NF- κ B-mediated transcription are not affected in SCC cell lines by VOPP1 knockdown. Taken together, these data support the hypothesis that VOPP1 overexpression in cancer participates in the control of the intracellular redox state, and that its loss leads to oxidative cellular injury leading to cell death by the intrinsic apoptotic pathway.

Laboratory Investigation (2011) 91, 1170–1180; doi:10.1038/labinvest.2011.70; published online 25 April 2011

KEYWORDS: apoptosis; cancer; overexpressed; oxidative stress; VOPP1

The *vesicular overexpressed in cancer prosurvival protein 1 (VOPP1)* gene product, previously known as GASP¹ and ECOP², has been shown to be upregulated in a number of human cancer types, including squamous cell carcinoma (SCC).^{3,4} Reports from our group⁴ and others² have shown that siRNA-mediated knockdown of VOPP1 in cell culture model systems results in cell death, consistent with the notion that VOPP1 overexpression has pro-survival effects in cancer biology. In certain experimental systems, results have suggested that VOPP1 may modulate the NF- κ B signaling axis;^{2,4,5} however, in a previous report, we had found that this association is not universal among cancer-derived cell lines.⁴ Moreover, the localization of the VOPP1 protein to intracellular vesicles³ makes the model of VOPP1 interaction with cytoplasmic NF- κ B proteins problematic. To further elucidate the mechanism of VOPP1 siRNA-mediated cell death in relevant cancer-derived models of VOPP1

overexpression, we report here a series of experiments that: (i) better characterize the apoptotic pathway induced by VOPP1 knockdown in human SCC cell lines, (ii) provide additional evidence that NF- κ B does not have a role in apoptosis caused by the loss of VOPP1 in SCC cells, and (iii) show that loss of VOPP1 results in changes in the intracellular redox state and in mitochondrial dysfunction, which result in the induction of apoptosis.

MATERIALS AND METHODS

Cell Culture and Nucleic Acid Transfection

SCC-9 (derived from head and neck SCC), FaDu (derived from head and neck SCC), H2170 (derived from lung SCC), and HeLa (derived from cervical adenocarcinoma) were grown in DMEM/F12 10% FBS, seeded in 96-well plates at 5000–10 000 cells per well, or in 24-well plates with glass coverslips at 25 000–30 000 cells per well. Annealed

¹Department of Pathology, University of Virginia, Charlottesville, VA, USA; ²Department of College of Arts and Sciences, University of Virginia, Charlottesville, VA, USA and ³Department of Biochemistry and Molecular Genetics, University of Virginia, Charlottesville, VA, USA

Correspondence: Dr AS Baras, Department of Pathology, University of Virginia, 3024 University Hospital, PO Box 800214, Charlottesville, VA 22908, USA.
E-mail: baras@virginia.edu

Received 8 November 2010; revised 2 March 2011; accepted 7 March 2011

double-stranded siRNA or plasmid DNA was introduced into cells using Lipofectamine 2000 (Invitrogen) according to the manufacturer's protocols 24 h after seeding.

RNA and Protein Isolation, PAGE, and Immunoblotting

These techniques were performed as reported previously.^{3,4} Primary antibody reagents were: affinity-purified polyclonal rabbit anti-VOPP1.⁴ Commercial primary antibodies employed were: (i) polyclonal rabbit anti-tubulin (Cell Signaling technologies, no. 2148) and (ii) monoclonal mouse anti-GAPDH (Ambion, no. AM4300).

VOPP1 Targeting siRNAs

Two siRNAs were designed targeting ECOP mRNA: the first in the coding sequence, 5'-GGACUCUAUCCAACCUAUU-3', and the second in the 3'-UTR, 5'-GACAGGAGAAGUACU GACU-3'. siRNA (5 or 20 pmol) was used in 96- or 24-well format, respectively. VOPP1 targeting siRNAs and GC content-matched siRNA controls were acquired from Invitrogen.

Trypan Blue Dye Exclusion Assay

A one part 0.4% Trypan blue staining solution (Gibco) was added to 10 parts cell suspension and cells were counted using a hemocytometer under microscopy.

Invitrogen LIVE/DEAD[®] Assay

Following VOPP1 siRNA knockdown in 96-well plates at 72 h post-siRNA transfection, cells were labeled with 1 μ M calcein AM (viable cell marker) and 2 μ M EthD-1 (dead cell marker) in culture media for 30 min. Cells were then directly imaged using an inverted fluorescent microscope using appropriate filter sets. Digital images were captured and then subsequently processed via ImageJ (NIH) image processing software (see Supplementary Material). Briefly, an index of cell death was constructed from the ratio of dead to live cell counts obtained, which was expressed as fold change relative to control.

Promega MultiTox-Fluor Assay

Following VOPP1 siRNA knockdown in 96-well plates at 72 h post-siRNA transfection, cells were incubated with two fluorescence substrates according to the manufacturer's protocols, glycyL-phenylalanyl-amino-fluorocoumarin (live cell protease substrate) and bis-alanyl-alanyl-phenylalanyl-rhodamine 110 (dead cell protease substrate). Specific fluorescence measurements for the live and dead signals were made using a fluorometer, and an index of cell death was constructed from the ratio of the dead to live signal, which was expressed as fold change relative to control.

Enzymatic Assays of Caspase-3/7 and Caspase-9

Luminescence-based Caspase-Glo 3/7 and Caspase-Glo 9 assays were performed in conjunction with the MultiTox-Fluor assay, as per the manufacture's protocols (Promega). The live cell signal from the MultiTox-Fluor assay was first

performed to normalize for cell number and then the lytic Caspase-Glo reaction was initiated and measured. Paclitaxel (Sigma, T7191) was used as a positive control to induce apoptosis via the intrinsic apoptotic pathway at 50 nM concentration.

Microarray Gene Expression Profiling

RNA samples from control and VOPP1 knockdown conditions were made into labeled probes and hybridized to Human Gene 1.0 ST Array (Affymetrix) using protocols, supplies, and equipment supplied or specified by the manufacturer at the UVA Biomolecular Research Facility. Expression values for each probe-set were generated using Affymetrix Power Tools Suite's PLIER algorithm with standard quantile normalization. To identify differentially expressed genes, we: (1) z-score normalized across conditions and (2) applied a minimum difference threshold (control *versus* knockdown) greater than 1.5 on the normalized scale and greater than 200 on the absolute expression scale. Random permutation testing was applied to assess how many genes would be identified using these criteria at random from the data.

Reporter Vector System Employed

pGL3-Con-hRluc (*constitutively active Renilla reporter*)

The luciferase gene, *luc* +, from the pGL3-Control vector was replaced by the updated version of the *Renilla* reporter gene, *hRluc*, from the pGL4.73 vector.

pGL3-minP-luc2 (*minimal promoter luciferase reporter*)

The luciferase gene, *luc* +, in the pGL3-Promoter vector was replaced by the updated version of luciferase, *luc2*, from the pGL4.20 vector.

pGL3-NF- κ B-luc2 ($5 \times$ NF- κ B and minimal promoter luciferase reporter)

The $5 \times$ NF- κ B element (TGGGGACTTCCGC) from pNF- κ B-Luc vector (Stratagene) was placed into pGL3-minP-luc2 described above upstream of the minimal promoter.

In this system, the pGL-3 backbone vector is kept common in all reporter vectors, thereby minimizing the potential of spurious effects due to differences in vector backbone sequences. The original vectors pGL3-Promotor, pGL3-Control, pGL4.73, and pGL4.20 were acquired from Promega (see Supplementary Material for cloning details).

NF- κ B Reporter Assays

Cells were seeded at a density of 5000–10 000 cells per well in 96-well plates. Reporter vectors (6 fmol of pGL3-minP-luc2 or pGL3-NF- κ B-luc2 and 3 fmol pGL3-Con-hRluc) and siRNAs (5 pmol) were transfected 24 h later. Luminescence was measured via the Dual-Luciferase[®] Reporter Assay System from Promega according to the manufacturer's protocols using a luminometer equipped with an onboard injector. Signal from the *luc2* reporters was normalized by the signal from the pGL3-Con-hRluc control vector and then converted

to fold change or percent change relative to the control condition of a given experiment.

ROS Determinations using CM-H2DCF-DA

Following VOPPI siRNA knockdown, cells grown on glass coverslips were labeled with 5 μM 5-(and-6)-chloromethyl-2',7'-dichlorodihydrofluorescein diacetate (CM-H₂DCF-DA) (Invitrogen) and 1 μM Hoechst 33342 (Invitrogen) in PBS for 30 min. Cells were then rinsed in dH₂O, returned to normal culture media, and imaged via fluorescence microscopy. Digital images were captured and then analyzed in ImageJ (NIH) with standard segmentation protocols to tabulate the total number of cells using the Hoechst stain as reference. The number of cells exhibiting significant CM-H₂DCF-DA signal was tabulated per condition examined using a constant threshold allowing for comparability. The percent of cells that were ROS positive was calculated for each condition examined.

Mitochondrial Viability using MitoTracker Red CMXRos

Following VOPPI knockdown, cells grown on glass coverslips were labeled with 100 nM MitoTracker Red CMXRos (Invitrogen) in PBS for 30 min. Cells were then returned to normal culture media and imaged live via fluorescence microscopy. Digital images were captured and then analyzed using the CellProfiler analysis suite (Broad Institute) to obtain per cell integrated intensity measures analogous to flow cytometry.

RESULTS

Validation of the Cell Culture Models Utilized to Study VOPPI Overexpression via siRNA-Based Loss of Function Studies

To determine if VOPPI overexpression is preserved in cell culture model systems of SCCs, we used immunoblotting to examine VOPPI protein expression in five SCC cell lines (SCC-9, SCC-25, FaDu, H157, and H2170) in comparison to benign (*n* = 4) and malignant (*n* = 9) human squamous tissue samples. HeLa cells were included to validate findings of previous literature. Data for the tissue samples along with SCC-9 and HeLa have been reported previously.⁴ As shown in Figure 1a, most cell lines (SCC-9, FaDu, H2170, and HeLa) exhibit VOPPI overexpression relative to benign squamous mucosa tissue samples and comparable levels to SCC samples. For this reason, we excluded the SCC-25 and H157 cell lines from further analyses given the experimental paradigm of employing siRNA to abrogate endogenous VOPPI overexpression developed below.

The effectiveness of the selected siRNA constructs for knockdown of VOPPI expression was next characterized in the cell lines shown to endogenously overexpress VOPPI. As shown in Figure 1a and b, a significant decrease in the level of VOPPI protein levels is achieved in all cell lines at 24 h post-siRNA transfection. The results for SCC-9 were quantified and indicated that on average the siRNA-based

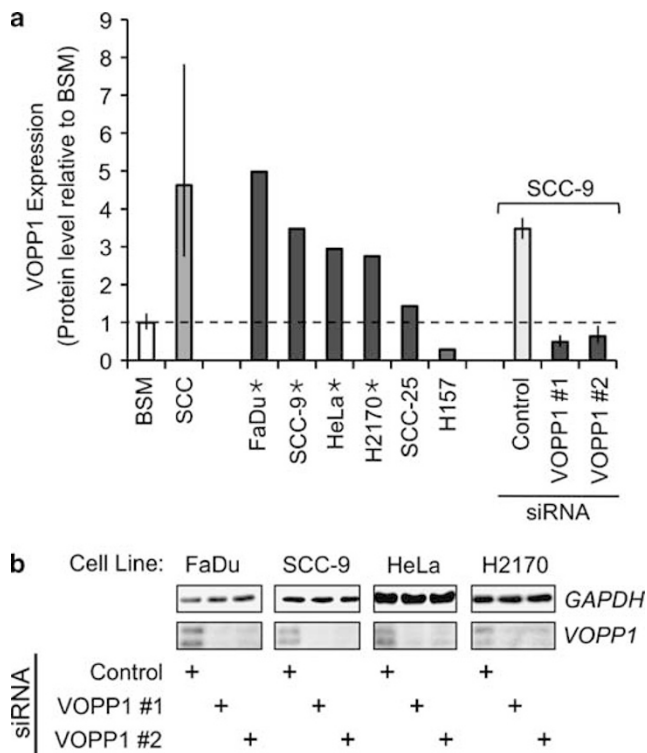


Figure 1 Vesicular overexpressed in cancer prosurvival protein 1 (VOPPI) expression in cell culture models of carcinoma and characterization of small interfering (si)RNA-mediated knockdown efficiency. (a) Quantification of VOPPI protein expression by densitometry of western blots, for benign squamous mucosa (BSM) samples (BSM, *n* = 4), squamous cell carcinoma samples (SCC, *n* = 9), and six cell lines (FaDu, SCC-9, HeLa, H2170, SCC-25, and H157). VOPPI protein quantitation from siRNA-mediated knockdown experiments in SCC-9 with two siRNA constructs (VOPPI nos. 1 and 2, *n* = 5 for each condition) are also shown. When present, error bars represent the 95% confidence intervals. The cell lines marked by asterisks show VOPPI expression at levels similar to the human SCC samples, which are elevated in comparison to the normal tissue of origin. The siRNA constructs decrease the level of VOPPI in SCC9 cells to levels similar to those in non-neoplastic tissue. (b) Representative western blots of the siRNA-mediated VOPPI knockdown 24 h post-siRNA transfection are shown. Both siRNA constructs are effective in reducing VOPPI expression in all cell lines tested.

approach was able to diminish VOPPI protein levels to 16% of controls.

VOPPI Knockdown Induces Cell Death at 72 h Post-Knockdown in Multiple Cell Culture Models of Cancer

We next characterized the effect of VOPPI knockdown on cell death over a 72-h time course in the SCC-9 cell line. As exhibited in Figure 2b, the knockdown of VOPPI results in a significant increase in the percentage of dead cells using the Trypan blue cell viability assay at 72 h post-siRNA transfection. These results are consistent with two different siRNA constructs targeting VOPPI, thereby reducing the chances that this is due to off-target siRNA effects. Figure 2a indicates that the knockdown at the protein level is evident at 24 h post-transfection and is stable throughout the course of

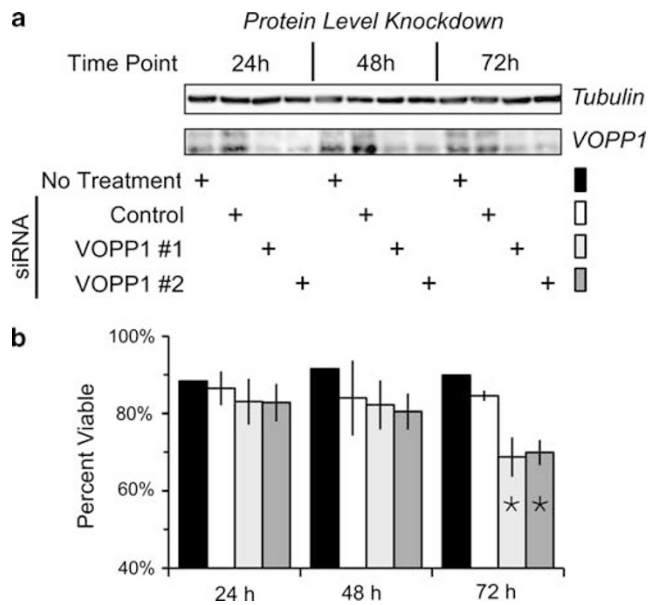


Figure 2 Time course of small interfering (si)RNA-mediated vesicular overexpressed in cancer prosurvival protein 1 (VOPPI) knockdown identifies that at 72-h post-siRNA transfection, VOPPI knockdown induces a decrease in the percentage of viable cells. **(a)** A western blot showing the extent of VOPPI protein reduction from siRNA-mediated knockdown in the squamous cell carcinoma (SCC)-derived cell line SCC-9 over a 3-day time course. **(b)** The percentage of viable cells as assessed by Trypan blue staining is shown over a 3-day time course of VOPPI knockdown; averages from two independent experiments are shown. The bar graphs are colored as shown in **(a)**. In both independent experiments, VOPPI knockdown induced a significant decrease in the percentage of viable cells at the 72 h time point, as assessed by Trypan blue staining; $P < 0.05$ from a two-proportion z-test (marked by asterisks). Error bars represent the standard error from two independent experiments. The data indicate that while VOPPI expression is effectively reduced by 24 h after transfection, a significant increase in cell death does not occur until 72 h after transfection.

the experiment. Thus, there is an approximate 48-h delay between cell death and VOPPI loss.

The cell death phenotype was evident by phase-contrast microscopy. This is illustrated for SCC-9 and HeLa cell culture in Figure 3a. With VOPPI knockdown, there are decreased numbers of adherent cells and an increased number of rounded-up cells, with shrunken, refractive nuclei. This morphology is consistent with cellular distress and death.

Cell death was additionally assessed by fluorescent microscopy of live and dead cells (LIVE/DEAD[®] assay; Invitrogen), wherein calcein-AM identifies live cells and ethidium homodimer-1 marks dead or damaged cells. In Figure 3b, this assay showed a consistent decrease in the number of viable cells as well as an increase in the number of dead or damaged cells when treated with both anti-VOPPI siRNA constructs as compared with control siRNA transfection. Representative microscopic fields with cell counts and fold changes of live/dead ratios are shown in Figure 3b. The quantified dead to live ratios from these experiments across the complete panel of cell lines utilized in this study, shown in Figure 3c, exhibit the consistent

phenotype of increased cell death with VOPPI knockdown at 72 h post-siRNA transfection. To further confirm these results, a third modality of cell death detection was employed, wherein the activities of specific proteases associated with living and dead cells are utilized to measure cells in culture directly and in a quantifiable manner (MultiTox assay; Promega). The results from the MultiTox assays, presented as fold changes in dead to live signal ratios (as was carried out with the microscopy-based assay), are shown in Figure 3d, again showing increased cell death in all cells with VOPPI knockdown. The sum total of all these experiments show that VOPPI siRNA-mediated knockdown consistently causes increased cell death after 72 h in multiple human cancer cell culture model systems.

VOPPI Knockdown Results in the Activation of the Classical Apoptotic Program through the Intrinsic Pathway

To determine if the increased cell death is due to the activation of the classical apoptotic program, the activation of caspase-3/7 was assayed. As shown in Figure 4a, VOPPI knockdown in SCC-9 cells results in caspase-3 proteolytic activation, indicating that an apoptotic response has been executed. The timing of this activation correlates well with the observed cell death phenotype: absent at 24 h post-knockdown and present at 72 h post-knockdown. In Figure 4b, these results are extended to the other cell lines in the panel, confirming that a consistent induction of apoptosis is observed with VOPPI knockdown at 72 h post-siRNA transfection.

Having established that VOPPI knockdown induces apoptosis, we next examined whether this was preceded by the activation of the intrinsic apoptotic signaling pathway, which can be monitored by the enzymatic activity of caspase-9, also referred to as apoptosome activation.⁶⁻⁹ Figure 4c shows that caspase-9 activity is activated within 48 h post-siRNA-mediated VOPPI knockdown, which is consistent with apoptosis being induced by the intrinsic pathway.

VOPPI Knockdown in SCC Cells does not Affect NF- κ B-Mediated Transcription

Previous experiments using HeLa and HEK cell lines associated VOPPI with NF- κ B signaling,² which we were able to replicate in HeLa cells, but not in SCC-9 cells.⁴ To extend these studies to other human squamous carcinoma-derived cell lines, we included FaDu and H2170 cells in these experiments, wherein we tested whether modulation of VOPPI expression could alter NF- κ B signaling. Figure 5a shows that decreased NF- κ B-responsive transcription only occurs in HeLa cells in response to VOPPI knockdown, but not in the three cell lines derived from human SCC. The data in Figure 5a represent the aggregate of five independent experiments each conducted in triplicate spanning the complete time course examined in this study (24, 48, and 72 h post-siRNA transfection). No individual time point exhibited significant changes in NF- κ B signaling with VOPPI

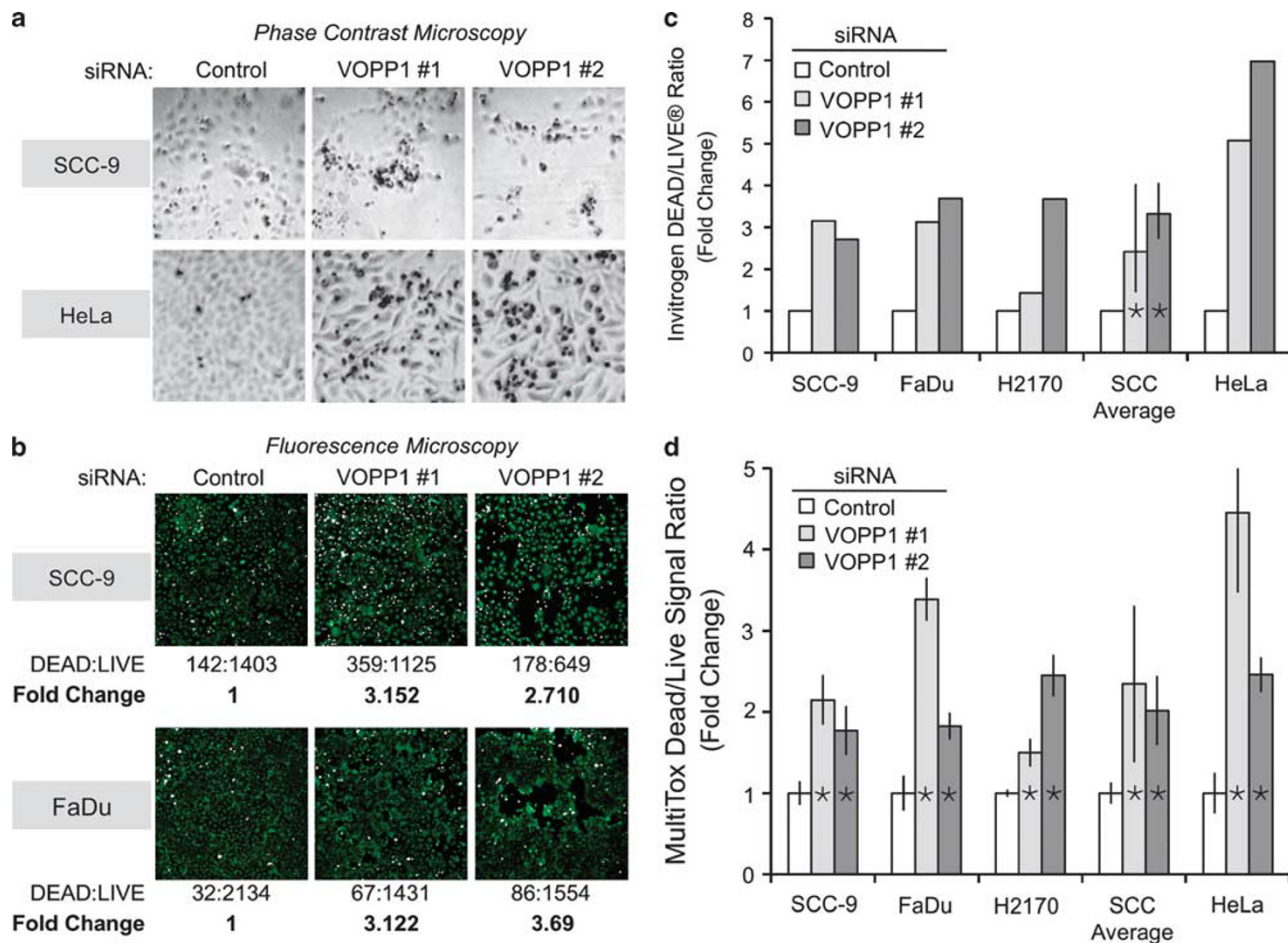


Figure 3 Vesicular overexpression in cancer prosurvival protein 1 (VOPP1) knockdown-induced cell death is evident at 72 h post-small interfering (si)RNA transfection by multiple detection modalities. **(a)** Phase-contrast images of squamous cell carcinoma (SCC)-9 and HeLa taken from VOPP1 siRNA knockdown experiments at 72-h post-transfection. **(b)** Fluorescence microscopy images from cells labeled with LIVE/DEAD[®] probes from Molecular Probes[®] during VOPP1 knockdown (72-h post-transfection) in the SCC-derived cell lines SCC-9 and FaDu. White signal indicates dead or dying cells and green signal indicates viable cells. Automated quantifications from the ImageJ software are included below each row of images. The results show that there is a significant decrease in the number of viable cells and an increase in dead or dying cells with anti-VOPP1 siRNA treatment compared with controls. **(c)** The quantified DEAD/LIVE[®] ratios expressed as fold change relative to the control siRNA condition per cell line, as depicted in **(b)**. The average fold changes observed in the three SCC-derived cell lines are also included, and show a significant increase ($P < 0.05$, one-sample one-tailed t -test for fold change greater than 1) in DEAD/LIVE[®] ratios from these aggregate data. **(d)** The results of the dead to live signal ratio from the MultiTox assay are shown expressed as fold change relative to the control siRNA condition for each cell line. Individual experiments for each cell line were conducted in triplicate. As in **(c)**, the average of the three SCC-derived cell lines is also depicted. All measures employed show a marked increase in cell death 72 h after siRNA transfection occurs with both VOPP1 siRNA constructs in all cell lines compared with a control siRNA construct, consistent with an induction of cell death specific to the reduction in VOPP1 expression. All error bars in this figure represent 95% confidence intervals and asterisks indicate $P < 0.05$.

knockdown (data not shown). We next examined if VOPP1 knockdown affects the ability of the cells to respond to a known NF- κ B stimulus (TNF α). The data presented in Figure 5b show that NF- κ B-mediated transcription induced by TNF α is unaffected by VOPP1 knockdown in SCC-derived cells. This indicates that VOPP1 knockdown does not abrogate NF- κ B signaling in these cell types to appropriate activating signals. These results are consistent with the hypothesis that altered NF- κ B signaling does not mediate the cell death phenotype observed in SCC due to the loss of VOPP1 overexpression.

Microarray Analysis of VOPP1 Knockdown Reveals Associations with Oxidative Stress and Mitochondrial Dysfunction

To obtain information that could point to a potential mechanism of cell death in SCC cell lines due to the loss of VOPP1 expression, we performed microarray gene expression profiling. The transcriptome in SCC-9 cells was queried at 48-h post-siRNA transfection because our previous data indicated that at this time apoptotic signaling is occurring based on caspase-9 activation, but cell death has not yet significantly occurred. As per our methods, 280 genes were identified as

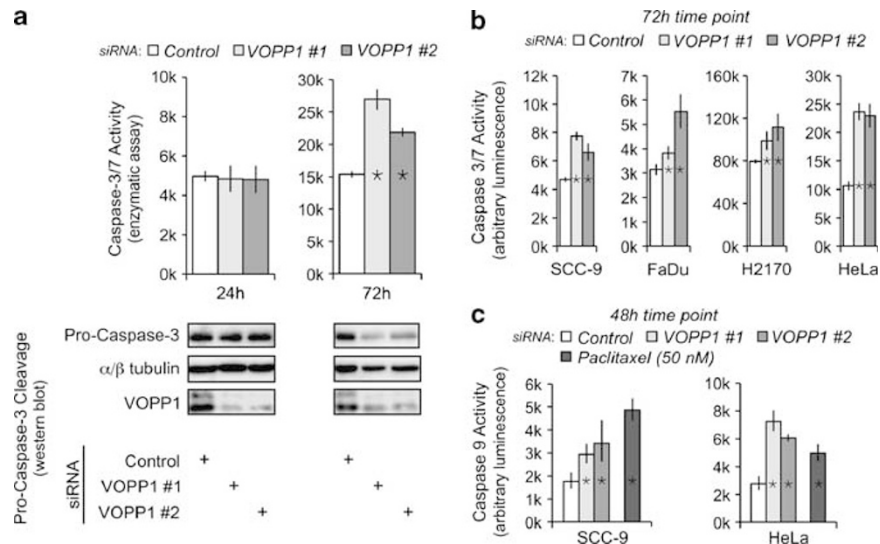


Figure 4 Vesicular overexpressed in cancer prosurvival protein 1 (VOPP1) knockdown-induced cell death is the result of the activation of apoptosis. (a) Results of enzymatic assays for caspase-3/7 in small interfering (si)RNA-mediated knockdown experiments in the squamous cell carcinoma (SCC)-9 cell line are shown in the upper panel. The data shown is the average of two independent experiments, conducted in at least quadruplicate each. Only 72-h time-point differences were significant ($P < 0.05$ marked by asterisks, Student's t -test). The lower panel shows pro-caspase-3 cleavage, followed by western blot at the same time points from an independent experiment. Both of these results indicate that a significant caspase-3/7 activation does not occur initially occur when VOPP1 expression is first reduced, but rather occurs at 72 h post-siRNA transfection. (b) Results of the enzymatic assays for caspase-3/7 activation in siRNA-mediated knockdown of VOPP1 are shown in multiple cell lines. The data represent independent experiments conducted in triplicate for each cell line noted. All cell lines show significant ($P < 0.05$ marked by asterisks, Student's t -test) caspase-3/7 activation only with VOPP1 targeting siRNA in relation to control at 72 h after transfection, which is coincident with the time point wherein cell viability was observed to decrease in earlier experiments. (c) Results of enzymatic assays for caspase-9 in siRNA-mediated knockdown experiments in SCC-9 and HeLa cell lines are shown. Paclitaxel is included as a positive control for the induction of apoptosis via the intrinsic pathway. The data indicate that caspase-9 activation by VOPP1 knockdown is observed 48 h after siRNA transfection. Data are from independent experiments conducted in triplicate for each condition noted. All error bars represent 95% confidence intervals with asterisks denoting significant differences for VOPP1 targeting siRNAs relative to control, $P < 0.05$ from a Student's t -test without assuming equal variances.

differentially expressed in cells undergoing VOPP1 knockdown versus control, $P < 0.005$ by random permutation, Figure 6a. This gene set was examined for enriched annotations using the Ingenuity pathway analysis tools (Ingenuity[®] Systems, www.ingenuity.com), using Fisher's exact test corrected for multiple testing (Benjamini-Hochberg false discovery rate). Two highly significant ($P < 0.01$) and interrelated annotations were associated with this gene set (Figure 6b). The first annotation identified is termed 'oxidative stress', and consists of genes/proteins involved in the response to oxidative stress and the maintenance of normal cellular redox states.¹⁰⁻¹³ The second annotation identified is termed 'mitochondrial dysfunction' and consists of genes/proteins whose malfunction could result in mitochondrial dysfunction.¹⁴⁻¹⁶ As confirmation of the significance of these findings, a gene list selected at random of equal size (280) was processed through Ingenuity[®] pathway analyses and no annotations were found to be significant ($P < 0.05$).

VOPP1 Knockdown Results in Increased Reactive Oxygen Species and Mitochondrial Dysfunction Before the Induction of Apoptosis

On the basis of the expression profiling results, the hypothesis was tested that VOPP1 knockdown would increase

reactive oxygen species (ROS) levels in cells before activation of the apoptotic cascade. Since the previous results showed that caspase activation had not yet occurred at 24 h post-VOPP1 knockdown, SCC-9 cells were assayed with the fluorescent ROS sensor 5-(and-6)-chloromethyl-2',7'-dichlorodihydrofluorescein diacetate at this time point. Figure 7a shows the resulting images from a representative experiment using the CM-H₂DCF-DA ROS sensor counterstained with DAPI, to serve as a reference. A clear increase in ROS levels is visually apparent in the VOPP1 knockdown conditions as compared with control, Figure 7a. The quantified results from five independent experiments using the CM-H₂DCFDA probe are shown in Figure 7b along with a positive control for this probe (treatment with 100 μ M H₂O₂ for 20 min). This evidence indicates that VOPP1 knockdown induces a highly significant ($P < 10^{-10}$) increase in ROS level, supporting the hypothesis generated from the microarray data.

As an increase in ROS may be related to oxidative injury of the mitochondria, we next examined whether VOPP1 knockdown would result in mitochondrial dysfunction at 24-h post-siRNA transfection. Mitochondrial viability was monitored by the per cell intensity of the mitochondrial selective dye MitoTracker[®] Red CMXRos (Invitrogen[®]). The accumulation of this dye, and therefore signal intensity, is

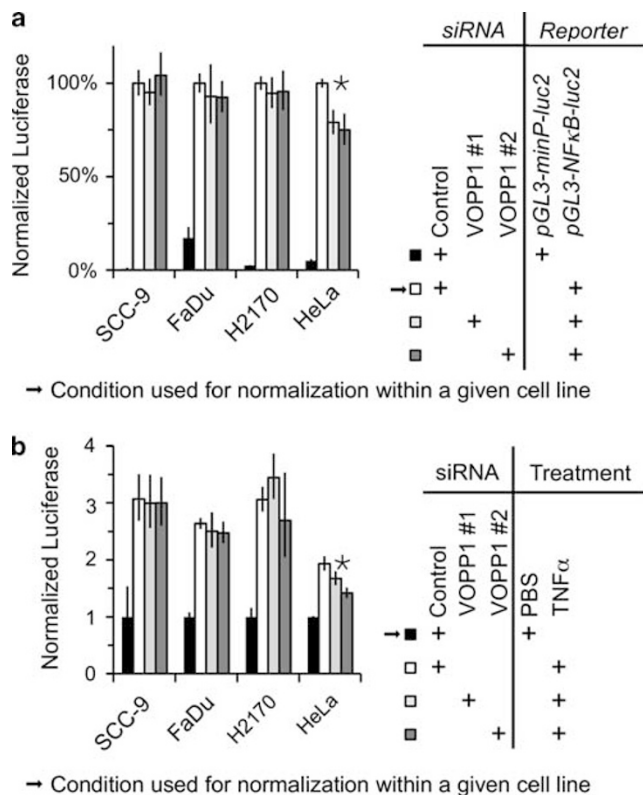


Figure 5 The nuclear factor (NF)- κ B signaling axis is not affected by the loss of vesicular overexpressed in cancer prosurvival protein 1 (VOPP1) expression in squamous cell carcinoma (SCC). **(a)** NF- κ B reporter activity is shown in four cell lines undergoing siRNA-mediated knockdown of VOPP1 expression. The data are the aggregate from five independent experiments each carried out in triplicate, and are presented relative to the condition of *pGL3-NF κ B-luc2* reporter/control siRNA per cell line. All cell lines exhibit a significant baseline NF- κ B-specific reporter activity. Only in the HeLa cell line did VOPP1 knockdown induce a significant decrease in baseline NF- κ B reporter activity. Three other cell lines derived from human SCC tumors did not show evidence of changes in NF- κ B reporter activity upon loss of VOPP1 expression. **(b)** NF- κ B reporter activity is shown in four cell lines undergoing siRNA-mediated knockdown of VOPP1 expression during the activation of the NF- κ B pathway by tumor necrosis factor- α (TNF α) treatment. Data are from two independent experiments conducted in triplicate for each SCC-derived cell line shown; measures of normalized NF- κ B activity are presented relative to the condition of *pGL3-NF κ B-luc2* reporter/control siRNA and phosphate-buffered saline (PBS) treatment per cell line, as indicated. TNF α stimulation did induce increased NF- κ B activity in all these systems as expected, but VOPP1 knockdown was only able to significantly abrogate this effect in HeLa cells. Thus, although the NF- κ B pathway is responsive in the three SCC cell lines, its activity is unaffected by changes in VOPP1 protein expression levels. All error bars represent 95% confidence intervals, with asterisks denoting significant differences for both VOPP1 targeting siRNAs relative to control; $P < 0.05$ from a Student's *t*-test without assuming equal variances.

dependent on mitochondrial membrane potential.¹⁷ As per our methods, using the CellProfiler image analysis software,¹⁸ we were able to quantify per cell total integrated fluorescence intensity in a manner analogous to flow cytometry, but allowing for the examination of live adherent cells. Figure 7c shows the images from a single experiment monitoring

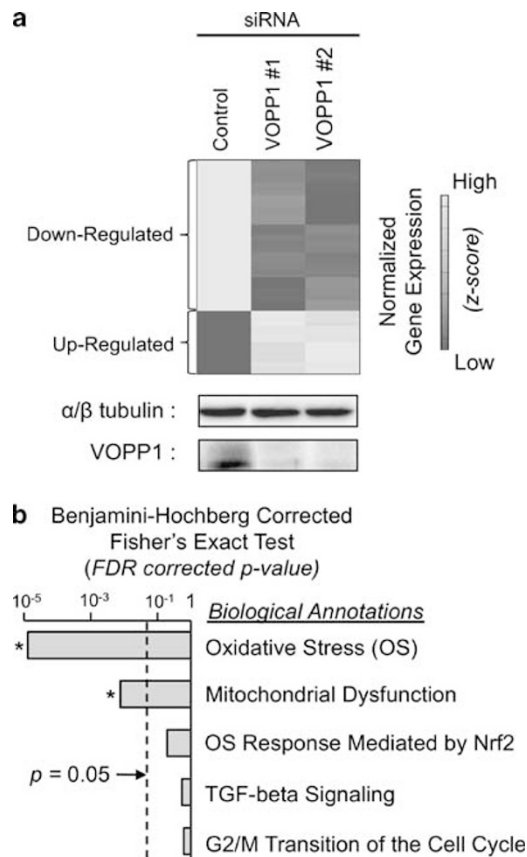


Figure 6 Transcripts whose expression levels are altered by vesicular overexpressed in cancer prosurvival protein 1 (VOPP1) knockdown at 48 h post-small interfering (si)RNA transfection are enriched for annotations pertaining to oxidative stress. **(a)** Heat map of the 280 genes identified as differentially expressed 48 h after VOPP1 knockdown in the squamous cell carcinoma (SCC)-9 cell line. Genes (columns) were cluster by Euclidean distance and unweighted pair group method with arithmetic mean (UPGMA). The western blot confirms VOPP1 protein level knockdown from the same biological samples assessed by microarray **(b)** The Ingenuity® Systems pathway analysis tool results are presented. A list of the top 5 annotations enriched in the set of differentially expressed genes with VOPP1 knockdown from **(a)**. The black vertical dashed line marks $P = 0.05$, with the asterisks marking significant ($P < 0.05$) results. Oxidative stress and mitochondrial dysfunction were identified as the most significantly altered gene expression annotations.

mitochondrial activity in VOPP1 knockdown. It is directly apparent that MitoTracker® Red CMXRos staining decreases with VOPP1 knockdown. In Figure 7c, the probability density estimates (analogous to histograms) of total per cell integrated fluorescence intensity are shown from two independent VOPP1 knockdown experiments, pooled together. A highly significant downward shift in intensities is evident with VOPP1 knockdown, Figure 7c and d, consistent with mitochondrial dysfunction. The significance of these findings was determined by a Kolmogorov–Smirnov test and the standard Student's *t*-test, both of which showed high levels of statistical significance, $P < 10^{-10}$, for both tests.

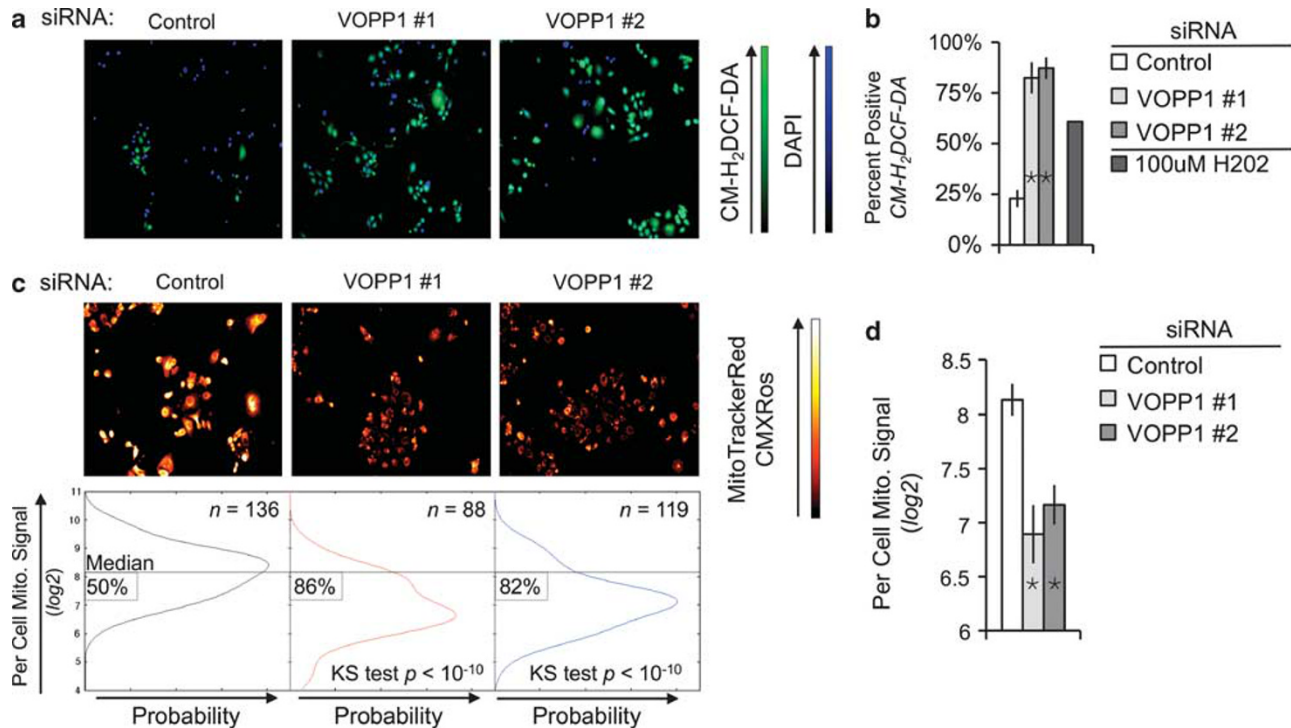


Figure 7 At 24 h post-small interfering (si)RNA transfection, vesicular overexpressed in cancer prosurvival protein 1 (VOPP1) knockdown induces oxidative stress, preceding the activation of apoptosis. **(a)** A representative set of images from VOPP1 knockdown in squamous cell carcinoma (SCC)-9, 24 h after transfection, analyzed by the reactive oxygen species (ROS) sensor 5-(and-6)-chloromethyl-2',7'-dichlorodihydrofluorescein diacetate (CM-H₂DCF-DA). Green color indicates the intensity of the ROS sensor's signal, whereas blue color from 4',6-diamidino-2-phenylindole (DAPI) serves as a reference to identify cells. All images were processed and scaled identically. At 24 h post-siRNA transfection, an increase in the percentage of cells with augmented ROS signal levels is directly evident. This coincides with a time point from previous experiments, wherein VOPP1 protein expression was reduced, but caspase activation and cell death had not yet occurred. **(b)** The percent CM-H₂DCF-DA-positive cells per field in five independent experiments are presented along with a positive control, 100 μ M H₂O₂ for 20 min is shown. Error bars represent the 95% confidence interval. Both VOPP1 targeting siRNAs induced a significant increase ($P < 10^{-10}$, Student's *t*-test) in percent ROS-positive cells. **(c)** Analysis of mitochondrial integrity 24 h after VOPP1 knockdown using MitoTracker Red CMXRos[®]. In the top portion, a representative set of images is shown, with all images scaled identically as indicated on the color bar. A decrease in signal intensity is visually evident from the data. In the bottom portion, the synthesis of two independent experiments showing the distributions of per cell signal intensities of the MitoTracker Red CMXRos[®] probe extracted using the CellProfiler analyses suite; *n* represents the total number of cells measured in each condition. The horizontal line represents the median per cell intensity of the control condition and the boxed percentage indicates what proportion of each condition was less than this value. The Kolmogorov-Smirnov tests (KS test) indicate a significant ($P < 10^{-10}$, marked by asterisks) downward shift in the distribution of signal with VOPP1 knockdown. **(d)** The same data from **(c)** is represented in standard bar graph format with 95% confidence intervals. Again, a significantly decreased signal is observed with VOPP1 knockdown ($P < 10^{-10}$ marked by asterisks, Student's *t*-test). This analysis indicates loss of mitochondrial integrity at a time point coincident with VOPP1 protein expression loss, but before caspase activation and cell death occur.

ROS are Required for Apoptosis in SCC Cells Induced by VOPP1 Knockdown

The previous results suggest that the increasing ROS levels observed after VOPP1 knockdown may be the cause of the induction of apoptosis seen at later time points. To test directly this hypothesis, the VOPP1 knockdown experiments were repeated in the presence of the thiol antioxidant *N*-acetyl cysteine (NAC) in the SCC-9 cell line. We hypothesized that NAC would abrogate the induction of apoptosis observed at 72-h post-siRNA transfection as it will quench the observed ROS generated from VOPP1 knockdown. Indeed, the induction of apoptosis observed with VOPP1 knockdown was significantly abrogated with 2.5 mM NAC (Figure 8a). To characterize this effect, the data are represented

as the percent of caspase-3/7 activation with NAC relative to baseline (no NAC) for each VOPP1 siRNA (Figure 8b). Caspase-3/7 activation with VOPP1 siRNA was significantly abrogated by approximately 50% with 2.5 mM NAC ($P < 10^{-4}$). We further hypothesized that if ROS production were the primary factor in the induction of apoptosis in this system, then the degree to which caspase activation was abrogated would be dependent on the dose of NAC. Figure 8c shows that this effect is in fact dose responsive with a strong Pearson's correlation of 0.792. From the regression, the slope of this linear association was found to equal -0.24 , indicating that for every 1 mM increase in NAC, on average a 24% reduction in the effect of VOPP1 knockdown is expected, with regard to the induction of apoptosis.

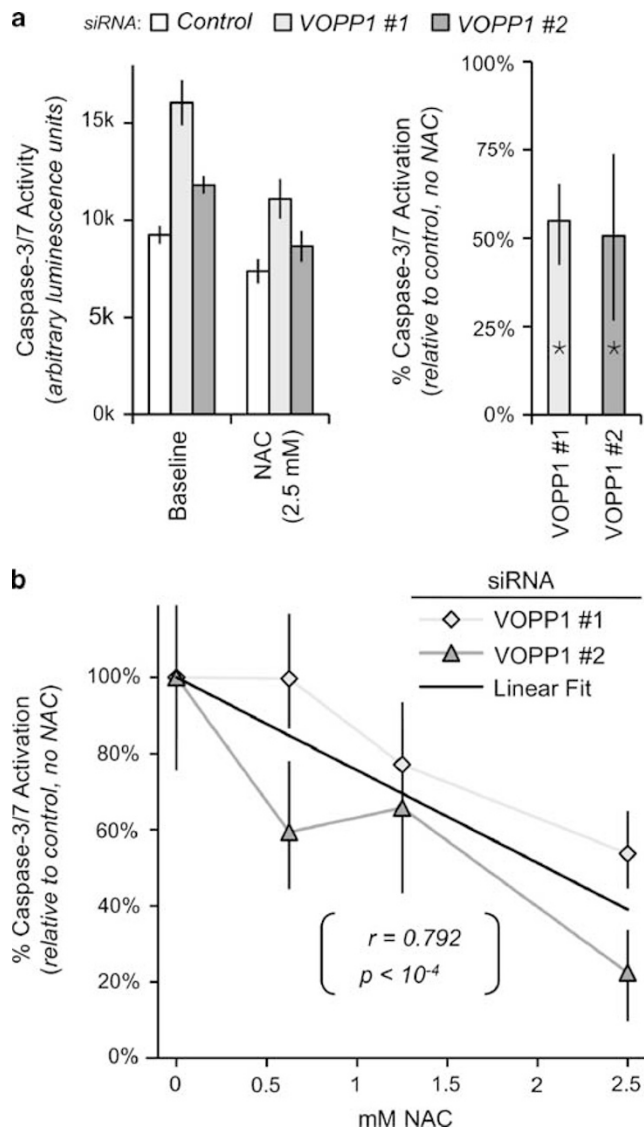


Figure 8 The induction of apoptosis from vesicular overexpressed in cancer prosurvival protein 1 (VOPPI) knockdown seen at 72 h post-siRNA transfection is abrogated with the use of the thiol-antioxidant *N*-acetyl cysteine (NAC) in a dose-dependent manner. **(a)** On the left axis, caspase-3/7 activity in arbitrary luminescence units is shown for control or VOPPI siRNAs with or without 2.5 mM NAC in squamous cell carcinoma (SCC)-9 cells. These data are from an independent experiment conducted in quadruplicate for all conditions. On the right axis, the normalized data for the two VOPPI small interfering (si)RNAs is re-plotted as percent caspase-3/7 activation relative to baseline (no NAC treatment). The asterisks denoted the significant decrease seen with both VOPPI targeting siRNAs ($P < 10^{-4}$, bootstrap analysis), indicating that the thiol antioxidant NAC can abrogate the induction of apoptosis observed with VOPPI knockdown 72 h post-transfection. **(b)** NAC is titrated from 2.5 mM down to zero and the percent caspase-3/7 activation, as in **(a)**, is shown relative to control, no NAC. These data are from an independent experiment conducted in sextuplicate for all conditions shown in **(b)**. The solid black line represents the linear regression of the trend observed in **(b)**, with Pearson's correlation coefficient (r) and corresponding P -value of significance (P) shown. The abrogation of VOPPI knockdown-induced apoptosis by NAC is dose responsive. All error bars in the figure represent the 95% confidence intervals.

DISCUSSION

It has been previously shown that VOPPI is overexpressed in gliomas and squamous carcinomas relative to their tissue of origin.²⁻⁴ Although this overexpression was originally ascribed to the *VOPPI* gene being co-amplified with the *EGFR* gene locus, we previously showed VOPPI gene amplification to be an infrequent event in squamous carcinomas.⁴ Interestingly, from analysis using the Oncomine database (Compendia Bioscience, Ann Arbor, MI, USA), the overexpression of this protein appears to be a well-conserved phenomenon in many other types of cancer, suggesting that higher levels of VOPPI expression may be selected for during tumorigenesis, and that transcriptional activation is indeed likely to be the most common mechanism for the elevated levels of this gene product.^{3,19}

That the increased levels of the VOPPI protein appear to be having a functional role in malignant cells has been supported by siRNA-mediated knockdown experiments in HeLa cells,² which has been validated in our laboratory.⁴ HeLa cells are derived from cervical adenocarcinoma, a relatively uncommon human neoplasm. We have extended this analysis to one of the most common human cancer types, squamous carcinomas arising in the lung and head and neck region. Fortunately, as shown in this and a previous report,⁴ there are several SCC cell lines that express VOPPI in levels that are similar to native carcinomas, and can serve as model systems to test the function of this protein. After having established that the chosen siRNA constructs were effective in reducing the level of VOPPI protein in these malignant cells to levels comparable to those found in benign squamous cells, our initial investigations indicated that elevated VOPPI levels indeed appear to be providing a function that, when lowered, makes SCC cells prone to cell death.

We confirmed that the loss of cells with VOPPI knockdown was indeed due to cell death by a variety of assays (vital dye exclusion by phase microscopy, LIVE/DEAD[®] fluorescence microscopy, and MultiTox live and dead associated protease levels). An important point of these investigations is that cell death is maximally induced by VOPPI knockdown at 72 h post-siRNA transfection, some 48 h after VOPPI protein has been significantly reduced. This delayed response suggests that VOPPI function may impact a cellular process that requires a significant amount of time to cause cell death.

The results presented here show that this cell death phenotype is the result of caspase-3/7-dependent apoptosis, which is being activated by the intrinsic (caspase-9) apoptosome formation pathway. A broad range of triggers including radiation, cytotoxic drugs, cellular stresses, and growth factor withdrawal are known to induce apoptosis through the intrinsic pathway.²⁰ Ultimately, many of these stressors damage the mitochondria by causing changes in the permeability of the membranes of this organelle,²¹ leading to cytochrome *c* release and apoptosome formation and activation.^{22,23}

To understand how VOPPI was activating apoptosis in SCC cells, we first turned to the hypothesis that VOPPI may

modulate NF- κ B signaling, a transcription factor that regulates the expression of genes relevant to apoptosis. In our model systems of carcinomas, we expect that activation of the NF- κ B pathway will be antiapoptotic as has been observed in very related model systems such as transformed human keratinocytes and the non-small-cell lung cancer cell line A549.^{24,25} Using an established NF- κ B-responsive promoter as a readout, we were able to verify some measure of decreased NF- κ B signaling in HeLa cells with VOPPI knockdown, as reported previously, but could identify no such effect in any of the three SCC cell lines. The lack of a direct effect on NF- κ B is not entirely surprising, as we have previously shown that VOPPI is localized to intracellular vesicular structures and does not exist as a free cellular cytosolic factor.³ This would argue against the hypothesis that the pro-survival phenotype that VOPPI overexpression confers onto cancer cells is mediated via direct modulation of the NF- κ B signaling axis, which occurs in the cytoplasm and nucleus. The fact that some association exists in HeLa cells may be an indirect secondary modulation of this pathway, which is cell-type specific, in response to other cellular process that are occurring owing to VOPPI knockdown.

Our initial efforts to discover clues pertaining to the cellular functions of VOPPI via sequence homology searches for potentially relevant functional domains were uninformative. Having failed to be able to deduce a function for VOPPI from first principles, the discovery-based approach of gene expression profiling proved profitable. The 48-h time-point post-siRNA transfection captured the transcriptome at a time when the intrinsic apoptosis signaling pathway was activated, but before cell death was maximally occurring, to sample the state of gene expression that was tilting the cells away from survival and towards cell death. The two significant associations of oxidative stress and mitochondrial dysfunction were particularly intriguing given that both of these interrelated factors are well-known triggers of the intrinsic apoptotic pathway.^{26–30} It therefore seems plausible that the apoptosis observed with VOPPI knockdown may be mediated, at least in part, by an increase in ROS associated with mitochondrial dysfunction, ultimately resulting in oxidative damage. This hypothesis also fits the observation that the apoptotic phenotype requires approximately 2–3 days to mature post-VOPPI knockdown, allowing time for ROS levels to rise and time for mitochondrial function to become sufficiently impaired to induce apoptosis. However, it is also possible that since intrinsic apoptotic signaling has already been activated at the 48-h time-point post-siRNA transfection, we may have captured the transcriptome at a point where changes in expression are not specific for VOPPI knockdown, but rather activation of intrinsic apoptotic signaling.

Fortunately, from the evidence presented in Figure 7, the hypotheses generated from the microarray data have proven to most likely be true. VOPPI knockdown induces an increased level of oxidative stress and mitochondrial dysfunction, as assessed by the CM-H₂DCF-DA and

MitoTracker[®] Red CMXRos, respectively. Importantly, these effects are observed at an early 24-h time-point post-siRNA transfection, wherein apoptosis and cell death are not evident. These cellular stressors are known to induce apoptosis through the intrinsic pathway,^{27,29–31} and we have shown that this form of apoptosis is activated with VOPPI knockdown. These results suggest that accumulating ROS levels might in fact be a trigger of the apoptosis observed at later time points. However, this is only a temporal association. The causal relationship between VOPPI knockdown-induced ROS levels and apoptosis was supported by the ability of the thiol-antioxidant NAC to abrogate the induction of apoptosis observed with VOPPI knockdown in a *dose-responsive* manner. This suggests that some *quantity* of oxidative stress develops with VOPPI knockdown and that it can be directly titrated away, which could explain as to why the induction of apoptosis required time (72 h) to fully develop. These findings support the notion that increased ROS levels in the cells mediate the apoptotic response observed with VOPPI knockdown.

The highly conserved nature of VOPPI overexpression in cancer observed in the Oncomine database,^{3,19} combined with its pro-survival phenotype evident in cell culture models of carcinomas,^{2,4} strongly implies that VOPPI overexpression provides the cells with functionalities that are advantageous. The investigations presented in this report have discovered that reducing VOPPI protein levels in carcinoma-derived cell lines results in oxidative stress, which eventually induces the execution of the apoptotic program. In addition, we have shown that the association between VOPPI and the NF- κ B pathway seen in HeLa cells is not universal and ultimately probably not the direct mechanism by which VOPPI overexpression exerts its pro-survival effects. The relatively abrupt (24 h post-siRNA transfection) induction of oxidative stress observed with VOPPI knockdown indicates that a source of oxidative stress is no longer being managed appropriately. Logical next steps stemming from these results would consider plausible sources of oxidative stress relevant to tumor biology and how VOPPI could aid in their neutralization. One likely candidate is the dysregulated metabolism common to cells that have undergone the neoplastic transformation. Of particular interest is the notion that mitochondrial functions such as oxidative phosphorylation become dysregulated in the neoplastic condition.^{32–39} VOPPI overexpression in neoplasia may function to somehow neutralize ROS that form as a by-product of dysregulated mitochondrial function, potentially through the vesicular structures to which this protein has been localized.³

Supplementary Information accompanies the paper on the Laboratory Investigation website (<http://www.laboratoryinvestigation.org>)

ACKNOWLEDGEMENTS

Alexander Baras is a member of the Biotechnology Training Program at The University of Virginia, supported by training Grant T32 GM008715 from the National Institutes of Health (USA). These studies were primarily

supported by a gift provided to the University of Virginia by Philip Morris (PM) USA. An External Advisory Committee oversaw the review and approval process without any affiliation with the University, PM USA, or any other tobacco company. Funding for this project was based on independent intramural and extramural reviews.

DISCLOSURE/CONFLICT OF INTEREST

The authors declare no conflict of interest.

- Eley GD, Reiter JL, Pandita A, *et al*. A chromosomal region 7p11.2 transcript map: its development and application to the study of EGFR amplicons in glioblastoma. *Neuro-oncology* 2002;4:86–94.
- Park S, James CD. ECop (EGFR-coamplified and overexpressed protein), a novel protein, regulates NF-kappaB transcriptional activity and associated apoptotic response in an IkkappaBalpha-dependent manner. *Oncogene* 2005;24:2495–2502.
- Baras A, Moskaluk CA. Intracellular localization of GASP/ECOP/VOPP1. *J Mol Histol* 2010.
- Baras A, Yu Y, Filtz M, *et al*. Combined genomic and gene expression microarray profiling identifies ECOP as an upregulated gene in squamous cell carcinomas independent of DNA amplification. *Oncogene* 2009.
- Matsuda A, Suzuki Y, Honda G, *et al*. Large-scale identification and characterization of human genes that activate NF-kappaB and MAPK signaling pathways. *Oncogene* 2003;22:3307–3318.
- Acehan D, Jiang X, Morgan DG, *et al*. Three-dimensional structure of the apoptosome: implications for assembly, procaspase-9 binding, and activation. *Mol Cell* 2002;9:423–432.
- Bao Q, Shi Y. Apoptosome: a platform for the activation of initiator caspases. *Cell Death Differ* 2007;14:56–65.
- Riedl SJ, Salvesen GS. The apoptosome: signalling platform of cell death. *Nat Rev Mol Cell Biol* 2007;8:405–413.
- Shi Y. Apoptosome: the cellular engine for the activation of caspase-9. *Structure* 2002;10:285–288.
- Carlsson H, Yhr M, Petersson S, *et al*. Psoriasis (S100A7) and calgranulin-B (S100A9) induction is dependent on reactive oxygen species and is downregulated by Bcl-2 and antioxidants. *Cancer Biol Ther* 2005;4:998–1005.
- Hoek JB, Pastorino JG. Ethanol, oxidative stress, and cytokine-induced liver cell injury. *Alcohol* 2002;27:63–68.
- Sawyer DB, Siwik DA, Xiao L, *et al*. Role of oxidative stress in myocardial hypertrophy and failure. *J Mol Cell Cardiol* 2002;34:379–388.
- Ziegelstein RC, He C, Hu Q. Hypoxia/reoxygenation stimulates Ca²⁺-dependent ICAM-1 mRNA expression in human aortic endothelial cells. *Biochem Biophys Res Commun* 2004;322:68–73.
- Keil U, Hauptmann S, Bonert A, *et al*. Mitochondrial dysfunction induced by disease relevant AbetaPP and tau protein mutations. *J Alzheimers Dis* 2006;9:139–146.
- Kim GJ, Chandrasekaran K, Morgan WF. Mitochondrial dysfunction, persistently elevated levels of reactive oxygen species and radiation-induced genomic instability: a review. *Mutagenesis* 2006;21:361–367.
- Lin MT, Beal MF. Mitochondrial dysfunction and oxidative stress in neurodegenerative diseases. *Nature* 2006;443:787–795.
- Poot M, Gibson LL, Singer VL. Detection of apoptosis in live cells by MitoTracker Red CMXRos and SYTO dye flow cytometry. *Cytometry* 1997;27:358–364.
- Carpenter AE, Jones TR, Lamprecht MR, *et al*. CellProfiler: image analysis software for identifying and quantifying cell phenotypes. *Genome Biol* 2006;7:R100.
- Rhodes DR, Yu J, Shanker K, *et al*. ONCOMINE: a cancer microarray database and integrated data-mining platform. *Neoplasia* 2004;6:1–6.
- Reed JC, Pellicchia M. Apoptosis-based therapies for hematologic malignancies. *Blood* 2005;106:408–418.
- Berridge MV, Herst PM, Lawen A. Targeting mitochondrial permeability in cancer drug development. *Mol Nutr Food Res* 2009;53:76–86.
- Kang MH, Reynolds CP. Bcl-2 inhibitors: targeting mitochondrial apoptotic pathways in cancer therapy. *Clin Cancer Res* 2009;15:1126–1132.
- Ledgerwood EC, Morison IM. Targeting the apoptosome for cancer therapy. *Clin Cancer Res* 2009;15:420–424.
- Kothny-Wilkes G, Kulms D, Poppelmann B, *et al*. Interleukin-1 protects transformed keratinocytes from tumor necrosis factor-related apoptosis-inducing ligand. *J Biol Chem* 1998;273:29247–29253.
- Lee KY, Chang W, Qiu D, *et al*. PG490 (triptolide) cooperates with tumor necrosis factor-alpha to induce apoptosis in tumor cells. *J Biol Chem* 1999;274:13451–13455.
- Decaudin D, Marzo I, Brenner C, *et al*. Mitochondria in chemotherapy-induced apoptosis: a prospective novel target of cancer therapy (review). *Int J Oncol* 1998;12:141–152.
- Fulda S, Debatin KM. Extrinsic *versus* intrinsic apoptosis pathways in anticancer chemotherapy. *Oncogene* 2006;25:4798–4811.
- Green DR, Kroemer G. The pathophysiology of mitochondrial cell death. *Science* 2004;305:626–629.
- Hengartner MO. The biochemistry of apoptosis. *Nature* 2000;407:770–776.
- Kroemer G, Reed JC. Mitochondrial control of cell death. *Nat Med* 2000;6:513–519.
- Boatright KM, Renatus M, Scott FL, *et al*. A unified model for apical caspase activation. *Mol Cell* 2003;11:529–541.
- Kroemer G, Pouyssegur J. Tumor cell metabolism: cancer's Achilles' heel. *Cancer Cell* 2008;13:472–482.
- Moreno-Sanchez R, Rodriguez-Enriquez S, Marin-Hernandez A, *et al*. Energy metabolism in tumor cells. *FEBS J* 2007;274:1393–1418.
- Moreno-Sanchez R, Rodriguez-Enriquez S, Saavedra E, *et al*. The bioenergetics of cancer: is glycolysis the main ATP supplier in all tumor cells? *Biofactors* 2009;35:209–225.
- Rodriguez-Enriquez S, Gallardo-Perez JC, Aviles-Salas A, *et al*. Energy metabolism transition in multi-cellular human tumor spheroids. *J Cell Physiol* 2008;216:189–197.
- Rosignol R, Gilkerson R, Aggeler R, *et al*. Energy substrate modulates mitochondrial structure and oxidative capacity in cancer cells. *Cancer Res* 2004;64:985–993.
- Warburg O. On the origin of cancer cells. *Science* 1956;123:309–314.
- Weber G. Enzymology of cancer cells (second of two parts). *N Engl J Med* 1977;296:541–551.
- Weber G. Enzymology of cancer cells (first of two parts). *N Engl J Med* 1977;296:486–492.